CNN based Mitotic HEp-2 Cell Image Detection

Krati Gupta, Arnav Bhavsar and Anil K. Sao
School of Computing & Electrical Engineering, Indian Institute of Technology Mandi, Mandi (HP), India

Keywords: Mitotic Cells, HEp-2 cells, Auto-immune Disorders, Computer-Aided Detection (CAD), CNN Architecture, Support Vector Machines, AlexNet Architecture.

Abstract: We propose a Convolutional Neural Network (CNN) framework to detect the individual mitotic HEp-2 cells against non-mitotic cells, which is important for Computer-Aided Detection (CAD) system for auto-immune disease diagnosis. The significant aspect of detecting mitotic HEp-2 cells is to consider the distinctive appearance differences between the mitotic and non-mitotic classes that are represented through the learned features from pre-trained CNN. We especially focus on gauging the effectiveness of learned features from different CNN layers, combined with traditional Support Vector Machine (SVM) classifier. We also consider the class sample skew between the classes. Importantly, we compare and discuss the performance of learned feature representations, and show that some of these features are indeed very effective in discriminating mitotic and non-mitotic cells. We demonstrate a high classification performance using the proposed framework.

1 INTRODUCTION

Indirect ImmunoFluorescence (IIF) imaging is considered to be a 'gold standard' to characterize the presence of Anti-Nuclear Antibody (ANA), in order to diagnose a connective tissue disorder i.e. autoimmune disorders (Kumar Y, 2009; Foggia et al., 2013; Hobson et al., 2016). Here HEp-2 cells are used as substrate, in which different antibodies on cells are visualized in form of distinct nuclear staining patterns in images and can be utilized to develop an efficient CAD system for aiding diagnosis. The prominent nuclear staining patterns show some significance in detection of staining patterns-specific antigens and the associated diseases. Due to subjective & semi-quantitative procedure, manual handling errors, intra-personnel and laboratory variations (Foggia et al., 2013; Hobson et al., 2014), the manual protocol of detection requires to be aided with a CAD system that can efficiently identify and detect the presence of staining patterns and associated diseases, in order to aid pathologists for obvious and non-ambiguous cases and reduce their work pressure.

The staining patterns generated on HEp-2 is based on the bonding between auto-antibodies to the cell components at different stages of the cell cycle. The staining patterns in a cell are visualized mainly in two cell cycle stages: interphase and mitosis stages (Tonti et al., 2015). As yet, most automated approaches have explored the classification schemes on dominant patterns of interphase stage (Hobson et al., 2016; Gupta et al., 2016; Gupta et al., 2014; Manivannan et al., 2016). However, the detection of mitotic type cells is also an important and principal step in HEp-2 screening framework (Miros et al., 2015) as the antigens released by the mitotic cells and their concentration are responsible for some lethal diseases. Also the identification of mitotic pattern cells is a beneficial indication for narrowing down the patient cell patterns. According to the literature, it is noticed that the mitotic cell detection problem can be addressed using the secondary counter-stain during staining procedure, which is not an economical process. Thus, in the present work, we primarily focus on the problem of mitotic cell detection, using only the primary counter-stain, which is itself a novel problem definition. Moreover, due to rare occurrence of mitotic samples, the sample imbalance between the mitotic and non-mitotic class during classification is also an important concern in this case. Therefore, for a complete screening system, it is crucial to consider mitotic phase cells also.

To the best of our knowledge, few authors have analyzed such mitotic cell detection problem for HEp-2 cases. For instance, in (Iannello et al., 2014; Foggia et al., 2010), authors have proposed a mitotic v/s interphase/non-mitotic cell classification criteria on a very less number of samples using morphological

Gupta, K., Bhavsar, A. and Sao, A.
CNN based Mitotic HEp-2 Cell Image Detection.
DOI: 10.5220/0006721501670174
In *Proceedings of the 11th International Joint Conference on Biomedical Engineering Systems and Technologies (BIOSTEC 2018) - Volume 2: BIOIMAGING*, pages 167-174
ISBN: 978-989-758-278-3

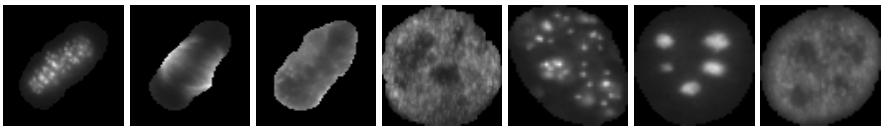

(a) (b) (c) (d) (e) (f) (g)

Figure 1: Some examples of cell images (a) to (c) mitotic cells & (d) to (g) non-mitotic cells.

and textural feature representation. In (Percannella et al., 2011), the authors have addressed the challenge of class sample skew or imbalance and have reviewed methods to handle the same. However, these approaches do not consider any standard publicly available dataset. In this work, we evaluate our approach using publicly available standard dataset, which would set a benchmark and help in comparative analysis of future studies.

In the proposed work, we focus on the classification of mitotic v/s non-mitotic cell images using features learned by a CNN. In current scenario of pattern recognition based works, CNNs have been proved to be efficient and reliable models to achieve remarkable performance for image classification and object detection tasks. Moreover, pre-trained CNN architectures can also perform an important role in terms of feature extractors. Hence, as a part of the work, we also analyze the effectiveness of features learned from different layers of the CNN. As we focus on considering the effectiveness of the features (and not on using a complex non-linear classification model), we use the features in a standard linear SVM, which is a popular linear classifier. In current work, we extract features from the layers of a pre-trained AlexNet architecture (Krizhevsky et al., 2012). The main contributions of the work are as follows:

(I) Generally, a visual clear distinction can be observed between the mitotic and non-mitotic classes. Such distinction can be seen in few examples of mitotic and non-mitotic cells, shown in Figure 1. Figures 1(a) to 1(c) are mitotic cells, while the remaining cells are non-mitotic. Considering this, we demonstrate that the learned feature representation through CNN layers can be effective in capturing such a distinction between the two types of cells, even when using the features from a CNN which is pre-trained on scene/object images. In this work, for the feature extraction task, we use the pre-trained AlexNet architecture.

(II) We also focus on an important aspect of the problem, i.e. class sample skew between the mitotic v/s non-mitotic classes, wherein the mitotic (i.e. the positive class) samples are very less in number, than non-mitotic ones. Hence, we apply two standard data skew handling strategies: undersampling and oversampling, and draw some useful insights.

(III) In addition to classification, we experimentally analyze the effectiveness of features learned at different CNN layers (low-level, mid-level and high-level features), and also provide a (standard) low-dimensional visual representation to support the experimental results.

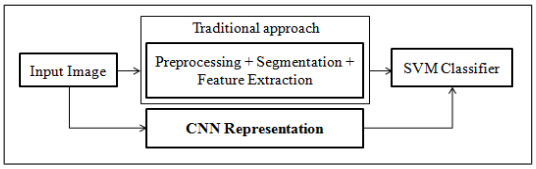

Figure 2: Block diagram of the traditional approach v/s CNN based classification approach.

(IV) In Figure 2, we have shown the block diagram of both a conventional and a CNN based classification approach. Traditional classification approaches typically involve steps such as pre-processing, segmentation and feature extraction task. Distortions in any of these tasks can accumulate and lead to inaccuracies. The proposed application of CNN is independent of pre-processing and segmentation. Here, the entire cell image is treated as input, while in case of traditional feature extraction approaches, the feature representation task is highly dependent on the selection of an appropriate Region-of-Interest (ROI) (e.g. (Iannello et al., 2014; Foggia et al., 2010)). Hence, such a work also demonstrates the usefulness of segmentation-free classification for cell images.

2 PROPOSED APPROACH

As mentioned earlier, we use the learned feature representation from CNN architecture for classification of mitotic v/s non-mitotic class samples and analyzing the effect of feature representation extracted from different layers of CNN. More specifically, the feature responses used in this work are from the conv1, conv2, conv3, conv4, conv5, and pool5 layers of a pre-trained AlexNet architecture. Thus we extract the feature representation of individual images from a CNN and then apply the same features in SVM, in order to get the better discrimination between the classes.

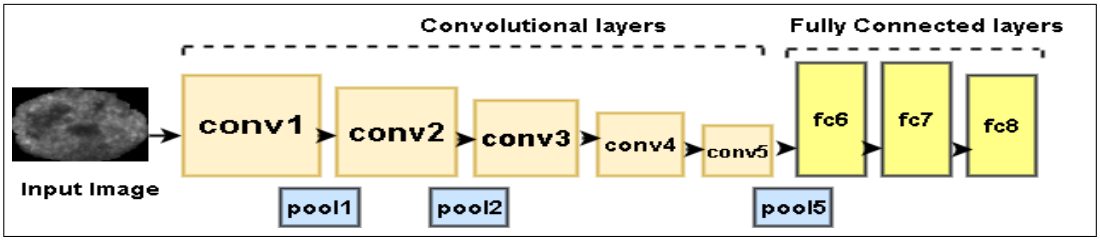

Figure 3: AlexNet architecture.

We now elaborate on the important aspects of our proposed approach.

2.1 Pre-trained CNN Architecture

Unlike the prior approaches for the mitotic vs non-mitotic classification task, we propose to use a CNN based feature representation scheme, in which the output responses of each layer are used as a generic feature representation. The idea of using CNN based features is motivated by its efficacy in various image processing and pattern recognition tasks (Xu et al., 2015; Sharif Razavian et al., 2014). We have used a publicly available pre-trained CNN architecture, i.e. AlexNet (Krizhevsky et al., 2012), trained on 1.3 million high-resolution images in the LSVRC-2010 ImageNet training set into the 1000 different object classes. Figure 3 shows the structure of the network. The network consists of 8 learned layers, including 5 convolutional layers with a kernel size varies from 3×3 to 11×11 and 3 fully connected layers. Rectified Linear Units (ReLU) is used as a non-linear activation function at each layer. Maxpooling kernels of size 3×3 are used at the different layers to build robustness for intra-class variations. We have used the pre-trained CNN architecture, that is trained on object images. Considering the 2D gray level images involved in the work, we use the 2D CNN. However, the proposed framework (including the CNN used) is not restricted to the input image dimension and can be extended in a straightforward manner for 3D input images also.

Also involving the visual differences in the two classes, we believe that the low-level or the higher-level features representation from such a pre-trained CNN can still effectively capture the discriminative information from cell images also. In section 3, we provide and discuss some activation maps to elaborate on this point, based on visualization of the feature representation. In Table 1, the details of layer types are given, along with the filter sizes and stride rates.

Table 1: Details in pre-trained AlexNet architecture.

	layer Type	Size
1	conv1 layer + ReLu	$96 \times 55 \times 55$
2	maxpool1	$96 \times 27 \times 27$, stride 2
3	conv2 layer + Relu	$256 \times 27 \times 27$
4	maxpool2	$256 \times 13 \times 13$, stride 2
5	conv3 layer + ReLu	$384 \times 13 \times 13$
6	conv4 layer + ReLu	$384 \times 13 \times 13$
7	conv5 layer + ReLu	$256 \times 13 \times 13$
8	maxpool5	$256 \times 6 \times 6$, stride 2

2.2 Layer-wise Features

Importantly, we consider the extraction of the output responses from different layers of CNN as low-level features, mid-level features and high level features representation. Hence, we use the output responses of layer conv1 with $96 \times 55 \times 55$ & conv2 with $256 \times 27 \times 27$ response as low-level feature representation, conv3 with $384 \times 13 \times 13$ as mid-level feature representation and similarly conv4 with $384 \times 13 \times 13$ & conv5 with $256 \times 13 \times 13$ output responses as high-level feature representation. Thus, we explore the layers for which we get a good representation for discriminating the input samples.

2.3 Classification Task

For classification task, we employ the traditional classifier i.e. Support Vector Machines (SVM). The SVM classifier can select very few optimal samples (the support vectors) to build the final model. Arguably, this aspect can be important in a scenario where we have less data (as is the case for the undersampling scenario in this work). Thus, we believe that the SVM can be a good choice of classifier, as we also later demonstrate. For SVM classifier, we chose the standard linear kernel instead of using any non-linear kernel. This is because of one of the purposes of this work is to gauge the effectiveness of different layers of CNN features, and a linear classifier would not transform features in any manner. Indeed, a linear

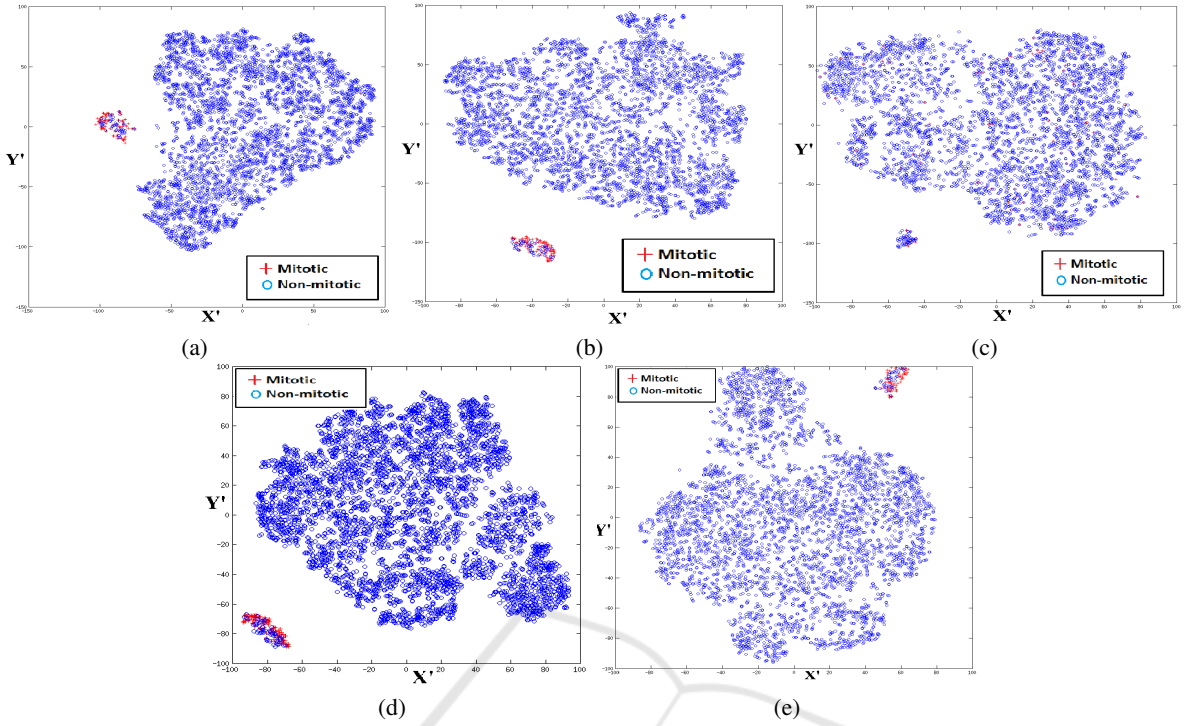

Figure 4: 2-D t-SNE-plot of high dimensional feature representation at (a) conv1, (b) conv2, (c) conv3, (d) conv4, and (e) conv5 (Better viewed in color or by zooming the images). The high dimensional feature representation is demonstrated in $(X^{'},Y^{'})$ space.

separation in features is indicated by the t-SNE plots (Van der Maaten and Hinton, 2008) of Figure 4 .

For comparison, we also perform classification using the same CNN architecture with Fully Connected (FC) layers. We treat this as a baseline classifier, and draw some useful insight from this comparison.

2.4 Data-skew

Considering a large amount of data skew between both the classes, we apply a well-known data skew handling techniques of undersampling and oversampling (for the case of the baseline CNN classifier). In the first case, we undersample the majority class samples in data space itself. Here, mitotic class images are the positive images with minority and non-mitotic is the majority class. Undersampling is done by randomly removing few samples from the non-mitotic class and equalizing the samples with the minority class. We demonstrate that most of our results are good even with undersampling. In the second case, an oversampling technique has also been tried for the same case, where oversampling of minority class samples are done using data augmentation with rotation. We rotate images in a range of angles between 0° to 150° in data space itself. In this case, the oversampling of minority class is done 40 times.

3 EXPERIMENTS & RESULTS

In this section, we describe about the dataset, experimental details, and results of the proposed approach.

3.1 Dataset Description

To validate our approach, we have used a publicly available dataset, i.e I3A Task 3 mitotic cell detection dataset (Vento, ; Foggia et al., 2013). It comprises of 100 mitotic cells and 4228 non-mitotic cells. All cells are accompanied with a ground truth or mask images. The mask images are provided to locate the cell nuclei region, though we have not used the mask image in our current work. The mitotic images are annotated as +1 and non-mitotic mask images as -1.

3.2 Experiment Details

For evaluation, we report the True-Positives (TP) and False-Positives (FP) accuracy. Mitotic class is considered as the positive class here. The F-score is also calculated for the results, which is the harmonic mean of precision and recall. Here, precision is defined as $\frac{TP}{TP+FP}$ and recall is $\frac{TP}{TP+FN}$ and FN denotes False Negatives.

We report results on a series of experiments that we conducted on different sets of training, testing and

Table 2: Experimental results of mitotic v/s non-mitotic classification. Here US & OS stand for undersampling and oversampling results respectively.

Layers	Training set (%)	Validation set (%)	Testing set (%)	TP acc. (%)	FP acc. (%)	Precision	Recall	F-score
Conv1	30	10	60	87.33	1.23	0.98	0.87	0.92
	40	10	50	90.60	1.14	0.98	0.90	0.94
	50	10	40	91.50	1.33	0.99	0.91	0.96
Conv2	30	10	60	90.17	1.13	0.99	0.90	0.94
	40	10	50	94.80	1.20	0.99	0.95	0.96
	50	10	40	95.00	1.24	0.99	0.95	0.97
Conv3	30	10	60	25.90	2.41	0.92	0.26	0.41
	40	10	50	35.60	3.62	0.91	0.36	0.52
	50	10	40	37.31	3.81	0.91	0.37	0.52
Conv4	30	10	60	98.33	1.14	0.99	0.98	0.98
	40	10	50	100	1.07	0.98	1.00	0.99
	50	10	40	100	1.08	0.99	1.00	0.99
Conv5	30	10	60	93.6	1.21	0.98	0.93	0.96
	40	10	50	98.8	1.21	0.98	0.98	0.98
	50	10	40	100	1.21	1.00	1.00	0.99
Pool5	30	10	60	93.60	1.10	0.98	0.93	0.96
	40	10	50	99.8	1.19	0.98	0.99	0.98
	50	10	40	100	1.10	0.99	1.00	0.99
Baseline-US	30	10	60	68.33	1.02	0.99	0.68	0.81
	40	10	50	76	1.04	0.99	0.76	0.8
	50	10	40	92.5	1.05	0.99	0.93	0.95
Baseline-OS	30	10	60	95	1.4	0.99	0.95	0.97
	40	10	50	98	1.14	0.99	0.98	0.98
	50	10	40	80	1.1	0.99	0.8	0.88

validation sets. The dataset is divided into different ratio of training, validation and testing sets that is clearly described in Table 2. In our experimentation, the entire dataset is divided into 3 experimental sets of 50%, 40% and 30% training sets and 40%, 50% and 60% testing sets respectively. The average results are reported over 10 random trials to maintain the robustness of the experimentation. In this way, each sample will once include in training, validation or testing set. In all experimentations, we have used 10% data samples for validation sets, in order to chose the best model and parameters settings. For classification, SVM classifier with standard linear kernel is used. For this, we have used the well known and efficient LIBLINEAR toolkit (Fan et al., 2008) with best chosen parameters.

3.3 Results

We report the TP, FP accuracy, precision, recall and F-score of all experiments in Table 2. The results are reported in form of low-level, mid and high level feature representation. As the networks is deep, so we consider the features from layers 4 and 5 as higher level features, those from layers 1 and 2 as lower level features and those from layer 3 as mid-level.

To visually show the discrimination between the classes and support our experimental results, t-SNE plots of higher dimensional feature representation of all the experiments are also presented in 2-dimensions (better viewed in color) in Figure 4. t-SNE is an approach to represent high dimensional data in 2-dimensions (Van der Maaten and Hinton, 2008).

Moreover, we also visualize the activation maps, i.e. feature maps of conv1 as low-level features, conv3 as mid-level features and conv5 as high-level feature representation in Figure 5 (Zeiler and Fergus, 2014), by using a deep visualization toolbox (Yosinski et al., 2015). The feature maps are shown for mitotic as well as for one non-mitotic cell class.

We observe that the classification accuracies of low-level feature representation and high-level representation are very high, even with very low amount of data due to undersampling (which obviates the need for oversampling in this case). The F-score values are more than 0.9 in most of the cases. On the other hand, the mid-level features show a very low accuracy suggesting that these are not discriminative enough.

We discuss more about the layer-wise performance along with some observations from the t-SNE plots and activation maps, and the comparison with the baseline CNN classifier, in the following subsections.

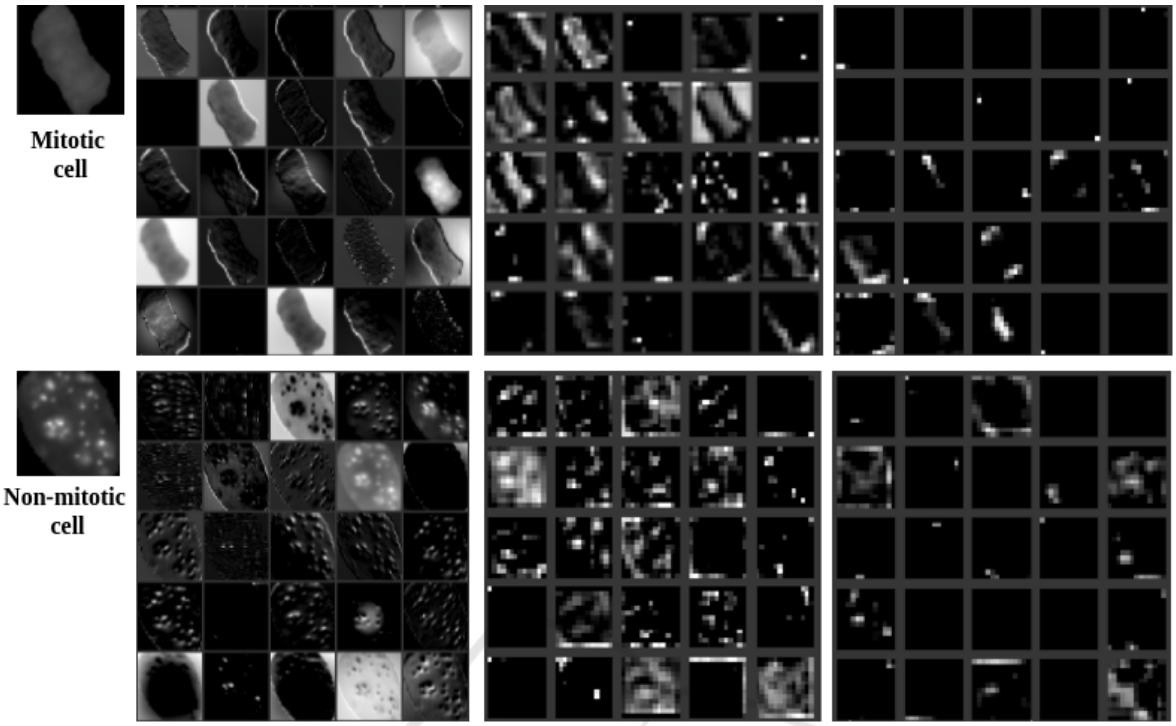

Figure 5: CNN-based feature extraction. Activation maps from Conv1 layer as low-level feature representation (2nd column), Conv3 as mid-level (3rd column) and Conv5 as high-level feature representation (4th column) are shown.

3.3.1 Conv1 and Conv2: Low-level Feature Representation

For low-level feature description, we extract the learned filter responses from conv1. Typically, the low-level representations exploits the intensity-based and some texture-based discriminative information. One can note that the classification results using conv1 and conv2 features are quite good. This indicates that the low-level intensity variation and texture information (as also observed in Figure. 1 images) can be effective for classification. The clear discrimination between samples is also observed in the t-SNE plot (Figures. 4(a) and 4(b)).

On the basis of visualization of activation maps examples from Figure 5 and classification results from Table 2, we observe that low-level feature representation are indeed clearly discriminative and represent the characteristics well. This is because the low-level features such as lines, edges, corners and dots or small blobs etc. are typically common to images irrespective of their domain. Thus, in this case, if there is discriminative information at the low-level such features are able to capture the same, even if the network is trained on object image data. Hence, we conclude that the AlexNet architecture, pre-trained on object images shows the feature representation, including the combinations of basic low-level entities in different sizes, shapes and textures, which are also quite useful for our classification task.

3.3.2 Conv3: Mid-level Feature Representation

We note the classification accuracies with conv3 features are quite low. As implied in some reported works (Oquab et al., 2014), the mid-level layer may require some re-training with respect to the cell images, as the pre-trained architecture is trained on a very different domain of images. Hence, the contextual information and feature representation is quite different and not discriminative for this domain of images.

We also note that we are employing a linear classifier, and as observed in the t-SNE plot (Figures. 4(c)), these features are not linearly separated, and may need non-linear models for better classification. In Figure 5, the activation maps of the feature responses from conv3 are shown. We observe that the features from conv3 across classes do not differ as clearly as in the case of low-level features. Thus, many filter may have irrelevant information, which may reduce the performance of classifier. Having said that, it is worth further exploring the interpretation of the mid-level features in this context.

3.3.3 Conv4, Conv5 and Pool5: High-level Feature Representation

With regards to the discussion above, this is an interesting case. We observe that the classification accuracies with learned features from conv4 and conv5 layers are very high. As for the low-level features, in this case too, the t-SNE plot (Figures. 4(d) and 4(e)) show a clear linear discrimination between the two classes.

Typically, these feature representation is known to incorporate more semantic information for object / scene images. However, for the cell image classification case, the images do not seem to have such high level semantic information, and the activation maps in Figure 5 seem to support this argument. Thus, while the activation maps are again not as clearly representative as those for low-level features, one hypothesis for the high performance is that the activation maps are also highly sparse. This could indicate that filter responses of irrelevant filters (in conv3) might be suppressed in high-level features and only few relevant filters might activated with discriminative responses. Again, as for conv3 responses, this is also worth exploring further to better analyze and interpret the performance of high-level features in this case.

3.4 Comparison with the Baseline CNN Classifier

Finally, we compare with the baseline CNN classifier wherein fully connected (FC) layers in the Alexnet are retrained for classification (Table 2). Note that both the baseline classifier and one case with the SVM classifier, operate on the pool5 features. Interestingly, in the undersampled case, the baseline classifier shows a much lower performance than the SVM classifier, especially with low-amount of training data. We believe that this is due to over-fitting, as the amount of data is low. As indicated earlier, the SVM classifier could be more robust here, as it effectively models the classifier using less number of samples. Typically, in many applications, the CNN classifier is trained with oversampled data. In the oversampled case, as the data size increases, the baseline CNN learns better and the accuracy increases. However, the note that the SVM operating on undersampled data performs equally well.

To the best of our knowledge, there are very few approaches proposed for this task, and indeed this is the first work on this dataset. Hence, we do not provide any comparisons with any other approaches. However, even in an absolute sense the best results achieved in this work are quite high and demonstrate that the approach is very effective to discriminate the mitotic and non-mitotic class samples.

4 CONCLUSION

In the proposed work, a mitotic cell detection framework for HEp-2 cell images is proposed via learned feature representation with a pre-trained CNN. We achieve high quality performance with low-level and high-level layered features of the architecture. Furthermore, we discuss some useful observations with respect to the features at various levels, and comparison with a baseline CNN. In future, we mean to build our own classification CNN architecture or re-train selected layers (transfer learning), which may also help in achieving better insights.

REFERENCES

Fan, R.-E., Chang, K.-W., Hsieh, C.-J., Wang, X.-R., and Lin, C.-J. (2008). LIBLINEAR: A library for large linear classification. *J. Mach. Learn. Res.*, 9:1871–1874.

Foggia, P., Percannella, G., Soda, P., and Vento, M. (2010). Early experiences in mitotic cells recognition on HEp-2 slides. In *2010 IEEE 23rd International Symposium on Computer-Based Medical Systems (CBMS)*, pages 38–43.

Foggia, P., Percannella, G., Soda, P., and Vento, M. (2013). Benchmarking HEp-2 cells classification methods. *IEEE Transactions on Medical Imaging*, 32(10):1878–1889.

Gupta, K., Gupta, V., Sao, A. K., Bhavsar, A., and Dileep, A. D. (2014). Class-specific hierarchical classification of HEp-2 cell images: The case of two classes. *2014 1st Workshop on Pattern Recognition Techniques for Indirect Immunofluorescence Images (I3A)*.

Gupta, V., Gupta, K., Bhavsar, A., and Sao, A. K. (2016). Hierarchical classification of HEp-2 cell images using class-specific features. In *6th European Workshop on Visual Information Processing, EUVIP 2016, Marseille, France, October 25-27, 2016*, pages 1–6.

Hobson, P., Lovell, B. C., Percannella, G., Saggese, A., Vento, M., and Wiliem, A. (2016). Computer aided diagnosis for anti-nuclear antibodies HEp-2 images: Progress and challenges. *Pattern Recognition Letters*, 82, Part 1:3 – 11. Pattern recognition Techniques for Indirect Immunofluorescence Images Analysis.

Hobson, P., Lovell, B. C., Percannella, G., Vento, M., and Wiliem, A. (2014). Classifying anti-nuclear antibodies HEp-2 images: A benchmarking platform. In *Proceedings of the 2014 22nd International Conference on Pattern Recognition*, ICPR '14, pages 3233–3238, Washington, DC, USA. IEEE Computer Society.

Iannello, G., Percannella, G., Soda, P., and Vento, M. (2014). Mitotic cells recognition in HEp-2 images. *Pattern Recognition Letters*, 45:136–144.

Krizhevsky, A., Sutskever, I., and Hinton, G. E. (2012). Imagenet classification with deep convolutional neural networks. In *Advances in Neural Information Processing Systems 25*, pages 1097–1105. Curran Associates, Inc.

Kumar Y, Bhatia A, R. M. (2009). Antinuclear antibodies and their detection methods in diagnosis of connective tissue diseases: a journey revisited. *Diagnostic Pathology*, 82, Part 1.

Manivannan, S., Li, W., Akbar, S., Wang, R., Zhang, J., and McKenna, S. J. (2016). An automated pattern recognition system for classifying indirect immunofluorescence images of HEp-2 cells and specimens. *Pattern Recognition*, 51:12 – 26.

Miros, A., Wiliem, A., Holohan, K., Ball, L., Hobson, P., and Lovell, B. C. (2015). A benchmarking platform for mitotic cell classification of ANA IIF HEp-2 images. In *2015 International Conference on Digital Image Computing: Techniques and Applications, DICTA 2015, Adelaide, Australia, November 23-25, 2015*, pages 1–6.

Oquab, M., Bottou, L., Laptev, I., and Sivic, J. (2014). Learning and transferring mid-level image representations using convolutional neural networks. In *Proceedings of the 2014 IEEE Conference on Computer Vision and Pattern Recognition*, CVPR '14, pages 1717–1724, Washington, DC, USA. IEEE Computer Society.

Percannella, G., Soda, P., and Vento, M. (2011). Mitotic HEp-2 cells recognition under class skew. In *Image Analysis and Processing – ICIAP 2011: 16th International Conference, Ravenna, Italy, September 14-16, 2011, Proceedings, Part II*, pages 353–362.

Sharif Razavian, A., Azizpour, H., Sullivan, J., and Carlsson, S. (2014). CNN features off-the-shelf: An astounding baseline for recognition. In *The IEEE Conference on Computer Vision and Pattern Recognition (CVPR) Workshops*.

Tonti, S., Di Cataldo, S., Macii, E., and Ficarra, E. (2015). Unsupervised HEp-2 mitosis recognition in indirect immunofluorescence imaging. In *Engineering in Medicine and Biology Society (EMBC), 2015 37th Annual International Conference of the IEEE*, pages 8135–8138. IEEE.

Van der Maaten, L. and Hinton, G. (2008). Visualizing high-dimensional data using t-SNE.

Vento, M. Benchmarking HEp-2 mitotic cell detection dataset, http://nerone.diem.unisa.it/hep2-benchmarking/dbtools/.

Xu, Z., Yang, Y., and Hauptmann, A. G. (2015). A discriminative CNN video representation for event detection. In *The IEEE Conference on Computer Vision and Pattern Recognition (CVPR)*.

Yosinski, J., Clune, J., Nguyen, A., Fuchs, T., and Lipson, H. (2015). Understanding neural networks through deep visualization. In *Deep Learning Workshop, International Conference on Machine Learning (ICML)*.

Zeiler, M. D. and Fergus, R. (2014). Visualizing and understanding convolutional networks. In *European conference on computer vision*, pages 818–833. Springer.